Sodium-Ion Batteries

*Michael D. Slater, Donghan Kim, Eungje Lee, and Christopher S. Johnson**

The status of ambient temperature sodium ion batteries is reviewed in light of recent developments in anode, electrolyte and cathode materials. These devices, although early in their stage of development, are promising for large-scale grid storage applications due to the abundance and very low cost of sodium-containing precursors used to make the components. The engineering knowledge developed recently for highly successful Li ion batteries can be leveraged to ensure rapid progress in this area, although different electrode materials and electrolytes will be required for dual intercalation systems based on sodium. In particular, new anode materials need to be identified, since the graphite anode, commonly used in lithium systems, does not intercalate sodium to any appreciable extent. A wider array of choices is available for cathodes, including high performance layered transition metal oxides and polyanionic compounds. Recent developments in electrodes are encouraging, but a great deal of research is necessary, particularly in new electrolytes, and the understanding of the SEI films. The engineering modeling calculations of Na-ion battery energy density indicate that 210 Wh kg^{-1} in gravimetric energy is possible for Na-ion batteries compared to existing Li-ion technology if a cathode capacity of 200 mAh g^{-1} and a 500 mAh g^{-1} anode can be discovered with an average cell potential of 3.3 V.

1. Introduction

Wide-scale implementation of renewable energy will require growth in production of inexpensive, efficient energy storage systems. The extension of battery technology to large–scale storage will become necessary as intermittent renewable energy generating technologies such as wind, solar, and wave become more prevalent and integrated into the electrical grid. While lithium-ion battery technology is quite mature, there remain questions regarding lithium battery safety, lifetime, poor low-temperature performance, and cost. Furthermore, as the use of large format lithium batteries becomes widespread, increasing demand for Li commodity chemicals combined with geographically-constrained Li mineral reserves will drive up prices.

Dr. M. D. Slater, Dr. D. Kim,
Dr. E. Lee, Dr. C. S. Johnson
Electrochemical Energy Storage Technologies
Chemical Sciences and Engineering Division
Argonne National Laboratory
9700 S Cass Ave, Argonne, IL 60439, USA
E-mail: cjohnson@anl.gov

DOI: 10.1002/adfm.201200691

The growing portable electronics market has resulted in skyrocketing sales of lithium ion batteries, equivalent to about US$ 7 billion worldwide in 2009.[1] About one-quarter of the world's production of lithium-containing precursor materials is now consumed by battery manufacture,[2] contributing to a steep rise in the price of Li_2CO_3 during the first decade of this century (**Figure 1**).[3] Widespread adoption of Li ion batteries for traction applications is expected to add to the pressure; in some scenarios, it is even predicted that lithium supplies will run out in the foreseeable future (**Figure 2**).[4] Supplies are likely to be even further constrained if these batteries are adopted for large-scale energy storage. Although new sources of lithium are currently being explored, and the metal can be recycled once enough large scale batteries have reached end-of-life, these avenues will likely lag behind demand, resulting in sharp short-term increases in price and associated fluctuations.

Based on the wide availability and low cost of sodium, ambient temperature sodium-based batteries have the potential for meeting large scale grid energy storage needs. In addition, since sodium is so abundant (4th most abundant element in the Earth crust), sodium-based batteries could provide an alternative chemistry to lithium batteries, and might become competitive to lithium-ion batteries in certain other markets. Supplies of sodium-containing precursors are vast, with huge reserves of 23 billion tons of soda ash located in the United States alone.[5] The abundance of resources and the much lower cost of trona (about $135–165/ton), from which sodium carbonate is produced, compared to lithium carbonate (about $5000/ton in 2010), provide compelling rationales for the use of sodium in large scale battery applications, particularly in the near-term.

Presently the options for stationary electrical storage consist of pumped-storage hydro, compressed air storage, advanced flywheels, thermal sinks, and batteries, including flow batteries and Li ion batteries.[6] All of the options have some drawbacks; for many of the battery systems, element toxicity (Pb, Cd) and high maintenance costs are issues, and in some cases, resource limitations are of concern, particularly considering the large scale of electrical grid load leveling.[7] Early research on Na metal based electrochemical energy storage systems focused on high-temperature Na/S and $Na/NiCl_2$ systems, both of which offer poor power density but useful energy densities at the

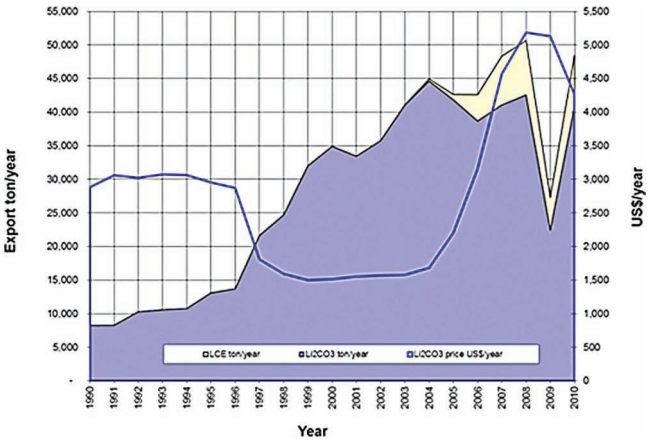

Figure 1. Fluctuation of the price and production of Li_2CO_3 over time. The sharp rise in price in the mid-2000s was caused in part by increases in demand for lithium batteries. Reproduced with permission.[3] Copyright 2012, The Lithium Site.

expense of complicated implementation. These devices operate at elevated temperatures (300–350 °C) to maintain the sodium in a liquid state and utilize solid ceramic electrolytes (most commonly β"-alumina). Their high energy densities, high round trip efficiency, and long cycle life make them attractive for load-leveling applications. However, the sophisticated engineering and materials needed to ensure durability and safety during high temperature operation drive up capital costs to about $500-600/kWh, well above the target of $250/kWh needed for widespread adoption.[8]

Recent developments in the field have drawn heavily on the technology developed in the past 20 years with Li ion batteries and thus electrode materials that offer good performance in non-aqueous, ambient temperature Na-ion cells are the focus of this paper with a primary emphasis on cathodes that are derived from layered transition metal oxides as sodium cation hosts. Recent information and results from the published literature are stressed, but older work is also discussed in this paper and some newest results from our lab are presented as examples.

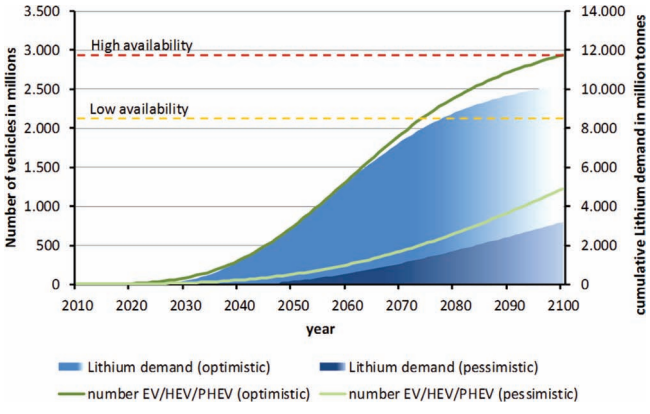

Figure 2. Lithium demand and availability and number of electric vehicles (EVs), hybrid electric vehicles (HEVs) and plugin hybrid electric vehicles PHEVs) over time. In low availability of lithium/optimistic EV/HEV/PHEV production scenarios, lithium could run out in the near future. Reproduced with permission.[4] Copyright 2012, Research Center for Energy Economics.

Michael Slater began his chemistry studies at DeAnza college and continued at the University of California, Santa Cruz (B.A. Mathematics and B.S. Chemistry, 2000). After receiving his Ph.D. in Chemistry (2009) from the University of California, Berkeley working on organic polymer based separations media, he joined Argonne National Laboratory as a postdoctoral researcher in the Electrochemical Energy Storage Group. His present research interests include multiplexed analytical techniques and energy storage in hybrid organic-inorganic systems.

Eungje Lee received his B.S. (1999) and M.S. (2003) degrees in Materials Science and Engineering from Seoul National University, and Ph.D. degree in Materials Science and Engineering from the University of Texas at Austin (2010) under the direction of professor Arumugam Manthiram. He is presently a postdoctoral researcher in the Chemical Science and Engineering Division at Argonne. His primary research interests include synthesis and structure-property relationships of materials for electrochemical energy storage/conversion systems.

Christopher S. Johnson is a staff chemist and project leader at Argonne National Laboratory, specializing in the research & development of battery materials and battery systems with 20 years of experience. His education background is the University of North Carolina at Chapel Hill (B.S. Chem.) and Northwestern University earning his Ph.D. in 1992. He has been active in the lithium and sodium battery materials field having published over 80 publications and 8 patents issued. His research interests are batteries for transportation and grid storage.

Table 1. Sodium versus Lithium characteristics.

Lithium	Sodium	Category
0.76	1.06	Cation radius (Å)
6.9 g mol^{-1}	23 g mol^{-1}	Atomic weight
0	0.3 V	E^o (vs. Li/Li^+)
$5000/ton	$150/ton	Cost, carbonates
3829	1165	Capacity (mAh g^{-1}), metal
Octahedral and tetrahedral	Octahedral and prismatic	Coordination preference

2. Na-Ion Energy Densities

In a dual intercalation system, the weight of cycleable Na or Li is a small fraction of the mass of all components, and capacities are determined primarily by the characteristics of the host structures that serve as electrodes. Thus, in principle there is not necessarily an energy density penalty in transitioning from a lithium ion battery to one based on sodium ions. Furthermore, sodium is somewhat less reducing than lithium (–2.71V vs. S.H.E., compared to –3.04 V) and the gravimetric capacity is lower (1165 mAh g^{-1} compared to 3829 mAh g^{-1}). Thus, devices based on metallic sodium anodes have lower energy densities and operating voltages than those with lithium metal anodes. A recent theoretical study by Ong, et al. compares similar materials operating in Li-ion and Na-ion systems.[9] These arise from a few fundamental differences between the two elements: the ~3x larger mass of Na, the larger ionic radius of Na (0.3 Å larger than Li; **Table 1**), and various thermodynamic parameters reflected in the ~300 mV higher standard reduction potential of Na. Successful reversible intercalation hosts must possess channels and interstitial sites large-enough to accept the larger Na^+ cation. Naturally, high ionic and electronic conductivity are also critically important. These facts indicate that practical systems will most likely need to utilize alternatives to metallic sodium, such as intercalation compounds or alloys, as anodes.

Since Na-ion batteries are an emerging technology, new materials to enable Na electrochemistry and the discovery of new redox couples has been relatively lacking. In sodium electrochemical systems, the greatest technical hurdles to overcome are the lack of high-performance electrode and electrolyte materials that are easy to synthesize, safe, non-toxic, long-lasting, and are low cost. Nevertheless, assuming that a high-capacity, dense Na-metal alloy can be used as the anode and a high-capacity cathode is employed, then it is possible to have an energy density that is comparable to current Li-ion battery systems. The model results for cell-level energy density are shown in **Figure 3**. In this sodium battery system model, the cell-level energy density calculations are made using a power to energy ratio of 2; this power to energy ratio is the long-term goal for full electric vehicle applications as suggested by the U.S. Advanced Battery Consortium. We assume an average discharge voltage of 3.3 V vs. Na/Na^+ for the cathode and compare different anodes such as Na metal, and Na_4Sn (903 mAh g^{-1}) at 0.25 V, Na_xC (200 mAh g^{-1} and 100 mAh g^{-1}) at 0.25 V. The average cathode voltage was lowered slightly with increasing capacity to account for observed experimental results. Standard Li-ion cell energy

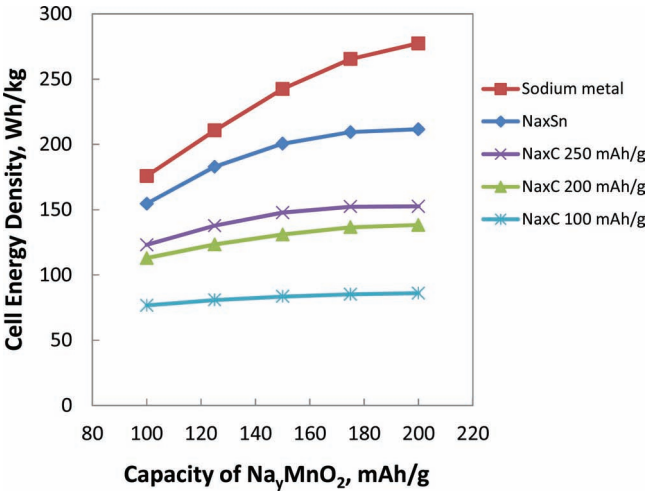

Figure 3. Energy densities for various Na-ion versus Li-ion battery systems calculated using the BatPaC model software package.

density calculated with the same technique range from 160 to 210 Wh kg^{-1} (marked in Figure 3). This modeling was done using the BatPaC v1.0 public domain model created by Argonne National Laboratory.[10]

For example, in the Na-Sn system, $Na_{15}Sn_4$ has a crystallographic density of 2.4 g cm^{-3}. The volume change going from Sn to $Na_{15}Sn_4$ is 424%, gravimetric capacity is 846 mAh g^{-1}, and it possesses extremely high volumetric capacity of 6164 mAh cm^{-3}. The volumetric energy density is much higher compared to the standard Li-ion anode material graphite (LiC_6; 818 mAh cm^{-3}). In addition, since Na does not alloy with Al, the Sn metal can be coated on lower cost Al current collectors instead of Cu. Also, having a charged metallic $Na_{15}Sn_4$ electrode may also improve safety, because the higher thermal conductivity of an active metal electrode will rapidly dissipate heat from the cell.

Our preliminary research indeed shows that it is possible to electrochemically react Na with Sn in an electrochemical cell at low voltages. **Figure 4** shows two-phase plateaus and the

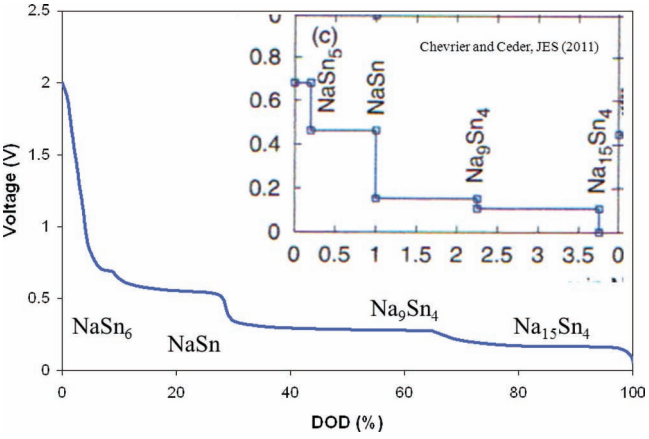

Figure 4. Na-Sn composition versus cell voltage for various Na-Sn alloy phases. Inset is the calculated phase diagram performed by Chevrier and Ceder. Reproduced with permission.[11] Cioyright 2011, The Electrochemical Society.[11]

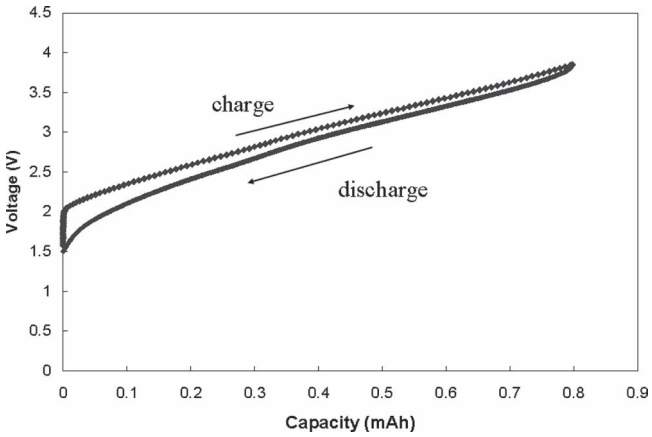

Figure 5. Cycle 21 voltage profile as a function of coin cell capacity of high-energy efficient non-aqueous Na-ion battery cell with layered transition metal oxide cathode and carbon anode: $Na_yC/Na_{1-y}(Ni_{1/3}Fe_{1/3}Mn_{1/3})O_2$ ($0 \le y \le 0.46$). A smooth intercalation reaction is observed indicative of a single phase solid-solution reaction.

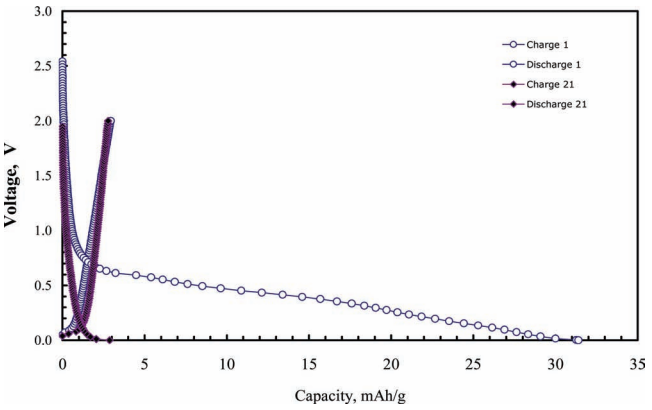

Figure 6. Na/C (graphite) cell showing lack of electrochemical activity. The electrolyte was 3:7 EC:EMC with 1 M $NaClO_4$.

corresponding Na-Sn compositions at various potentials. The average voltage for the full reaction is about 350 mV. This result strikingly compares favorably to DFT calculations conducted by Chevier and Ceder (see Figure 4 inset).[11] The highest capacity phase, $Na_{15}Sn_4$, exists in this system and possesses a voltage of about 200 mV vs. Na metal.

Metrics guiding the progression of battery technologies through their application are factors rooted in the thermodynamics and mechanism of charge storage (energy density, electrode reversibility and stability, the kinetics of the reaction) balanced by the basic tenets of cost: material abundance, synthesis and processing, and safety. High per-cycle energy efficiency is particularly important in grid-type energy storage, because wasted energy during peak-time increases overall generating costs. For example, in **Figure 5**, a secondary Na-ion cell using a Na-based layered oxide cathode material, $Na(Ni_{1/3}Fe_{1/3}Mn_{1/3})O_2$ coupled with carbon anode shows excellent energy efficiency as observed by the small voltage difference on charge versus discharge at a C/7 rate (13 mA g^{-1}).[12] While the result in Figure 5 is encouraging, the low specific capacity of the cathode is 91 mAh g^{-1} with an average cell voltage of 3.0 V, and therefore the corresponding energy density is too low, being 273 Wh kg^{-1} (active materials only).

3. Na Battery Anode Materials

Identification of a suitable negative electrode is the critical issue for the successful development of a sodium-ion battery and the area where analogy to Li-ion systems is the least applicable. Compared to lithium metal anodes, devices based on metallic sodium have lower theoretical energy densities due to the lower specific capacity (1166 mAh g^{-1}) and higher standard reduction potential of Na. The high reactivity of metallic sodium with the organic electrolyte solvents and dendrite formation during Na metal deposition are even more problematic than with Li metal anodes, while the low melting point of Na (98 °C) presents a significant safety hazard in devices designed for use at ambient temperatures using a Na metal electrode. Hence, it is critical to use a true Na-ion system, that is, one where Na ions are cycled back and forth from host electrodes in a 'rocking-chair' format. This design avoids the use of dangerously reactive Na metal. Unfortunately, it is very difficult at this early juncture in the field to make full cells, and, instead, most studies have only explored the electrochemical performance of new electrodes and materials used with Na metal in half cells.

3.1. Carbon-Based Anode Materials

Graphite, the most commonly used anode in lithium ion cells, does not intercalate sodium to any appreciable extent and is electrochemically irreversible as shown from the low capacity and irreversibility of a Na/C(graphite) cell in **Figure 6**.[13] Many other non-graphitic anodes that consist largely of various carbonaceous materials have been demonstrated to insert Na, such as petroleum cokes,[14–16] carbon black,[17] pitch-based carbon-fibers,[18] and polymers (poly(*para*-phenylene)).[19,20]

Hard-carbons, that is, generalized carbon materials that are synthesized at high-temperatures (~1000 °C, inert atmosphere) from carbon-based precursors have been more comprehensively modeled,[21,22] characterized,[23] and thermally tested in Na batteries.[24] These non-graphitic, but graphene containing, carbonaceous materials are considered the "first-generation" anode of choice for Na-ion systems. Raman spectra of various carbons are shown in **Figure 7**. It is clear that graphite (trace a) has a strong and narrow band (symmetric –C=C– stretch) at 1580 cm^{-1}, while the hard carbon material (trace c) resembles the Raman spectrum of glassy carbon (trace b) which bears an additional peak at 1350 cm^{-1} allowed by the increased disorder. Glassy carbon contains a turbostratic conglomeration of carbon particles densely packed together.

The voltage profile for non-graphitic carbon shows two distinct features: a sloping region below 1 V followed by low voltage intercalation reaction plateau below 100 mV with an overall first discharge capacity of 300 mAh g^{-1} (**Figure 8**). Notice that the electrochemical reaction is maintained above the point

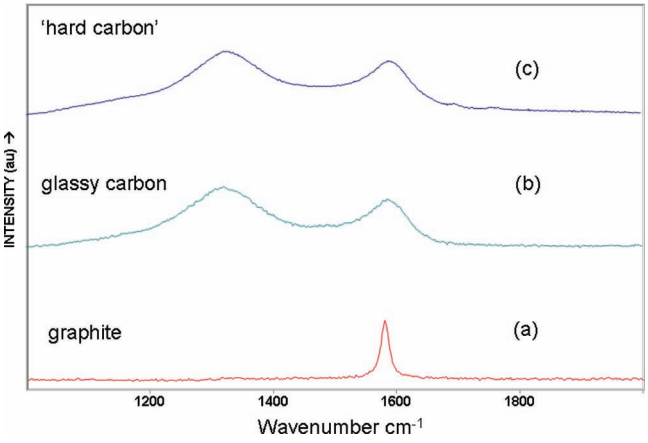

Figure 7. Raman specta of (a) graphite, (b) glassy carbon, and (c) the 'hard carbon' used in the full cell study shown in Figure 5.

where Na would plate at 0 V (inset, Figure 8). Also, there is a minimal amount of irreversible capacity loss in the first cycle (~17%), but cyclability afterwards is quite reasonable achieving a reversible total of about 220 mAh g^{-1}. This material has a low BET surface area of 3.3 m^2 g^{-1}, which from the literature, appears to be an important factor in achieving good reversible cycling of Na. For example, high-temperature (950 °C in Ar) pyrolysis of a resorcinol-formaldehyde resin produces carbon microspheres that are devoid of graphitic character, are nanocrystalline, exhibit low-porosity and low BET surface area (3 m^2 g^{-1}).[25] They contain individually stacked graphene layers that have a repeat unit of 2.2, and from the detailed analysis of the XRD pattern, a 31 Å spacing between the individual graphene sheets. These materials show a reversible 280 $mAhg^{-1}$ capacities in Na cells. The mechanism of the electrochemical reaction of Na with carbon was studied by ^{23}Na NMR. Two reversible (as a function of charge-discharge voltage) peak resonances are present which suggests two independent sites or interaction points with Na cations. First, a narrow resonance occurs at

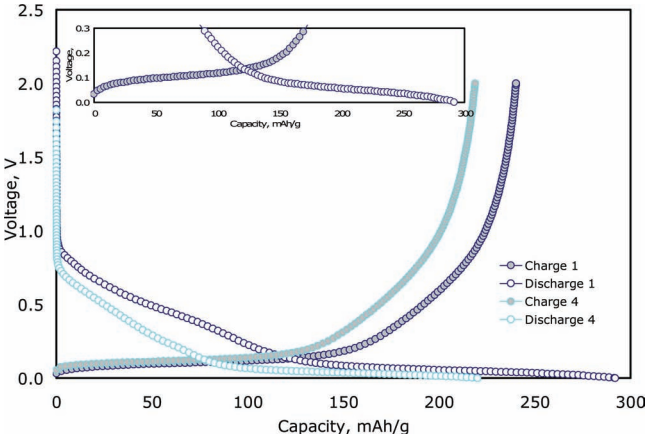

Figure 8. Na/C (carbon (non-graphitic)) voltage profiles number 1 and number 4. The electrolyte was 3:7 EC:EMC with 1 M $NaClO_4$.

+9 ppm which is ascribed to Na with more ionic character from its interaction with misaligned graphene layers in the carbon framework. The broader resonance between –20 and –30 ppm occurs at lower voltages (< 0.4V, and continuing below 0.2 V) is ascribed to a Na containing surface film with high diffusion character together with Na that is inserted into nanocavities. Most of the reversible capacity of the carbon microspheres therefore occurs in nanocavities. This work serves to remind us that the role of nanocavities and/or nanopores for Na insertion into carbon is important. It resembles the Na filling of pores in a "stack-of-cards" initially proposed by Stevens and Dahn and was later confirmed by in situ small angle X-ray scattering experiments by the same group.[22,26] The measurement showed that the mechanism of pore filling occurs at lower voltages, while at higher voltages the electrochemical reaction mechanism is ascribed to insertion of Na between graphene layers by intercalation. In general, electroactive and favorable carbons possess properties such as a small particle size, a low surface area/volume ratio and a morphology (such as spherical shape) that minimizes side-reactions with electrolyte at low voltages. Several attempts to improve the properties of hard carbon anodes have also been made, such as nanotemplating.[27]

3.2. Metal Oxide Anode Materials

There are relatively few non-carbonaceous Na intercalation type anodes. These are primarily early transition metal oxides and the sodium insertion potentials for most of them are too high to be of practical use. The lowest intercalation potential for sodium reported to date is for the sodium titanate $Na_2Ti_3O_7$, which provides 178 mAh g^{-1} at 0.3 V.[28] TiO_2 has also been examined in the form of amorphous nanowires;[29] *ca.* 0.4 Na can be reversibly cycled with an average potential of 1.5 V vs. Na/Na^+. It was found that a pseudocapacitance mechanism was responsible for the charge storage. Because of the size of solvated Na^+ cations, only large diameter amorphous nanotubes (> 120 nm) can support electrochemical cycling with sodium ions. These electrodes achieve their full capacity after several cycles, reaching a reversible capacity of 150 mAh g^{-1}. A high rate capability is observed with this system as a Na-ion battery when this anode material is coupled with one of our Na-ion cathode materials (*vide infra*) to produce secondary Na-ion cells. With two highly-stable intercalation electrodes, extended cycling of the Na-ion battery with no capacity fade is possible as shown in **Figure 9**, thus demonstrating the viability of Na-ion batteries as reversible, high power energy storing devices.

Conversion reactions of metal oxides have been demonstrated to be useful for Na-ion anodes. The concept was first demonstrated with the spinel $NiCo_2O_4$ which was found to provide ~ 200 mAh g^{-1} of reversible capacity after an initial discharge of 600 mAh g^{-1}.[30] A subsequent EXAFS study demonstrated that the conversion reaction to form sodium oxide (Na_2O) is the principal reaction because $NiCo_2O_4$ spinel cannot fit Na into its empty T_d site. This compound was also assembled into full cells against excess $Na_{0.7}CoO_2$; an improvement in the reversible capacity of the anode material was observed which serves as an important reminder in screening materials for Na-ion batteries: sodium metal behaves rather poorly as a

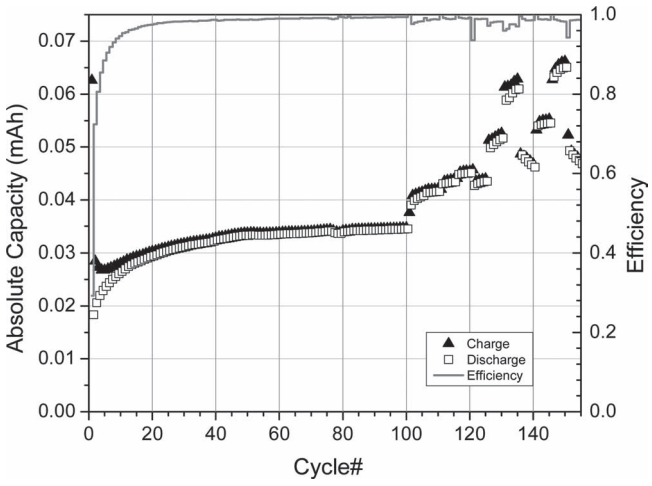

Figure 9. Extended cycling of a TiO_2 | NaPF6, EC/EMC | $NaLi_{0.2}Ni_{0.25}Mn_{0.75}O_{2.35}$ cell; the increases in capacity after cycle 100 are due to expansion of the operating voltage window.

counter electrode. The conversion reaction of Sb_2O_4 thin films was reported recently by Sun, *et al.*[31] In this case, reduction of the metal oxide is followed by alloying (to form Na_3Sb) and thus a very high reversible capacity of 800 mAh g^{-1} was demonstrated for over 20 cycles, at an average potential of 0.5 V vs. Na/Na^+.

3.3 Intermetallic Anode Materials

A study of SnSb/C nanocomposites as anodes for Na-ion batteries was recently published.[32] This work is an excellent example of the use of multicomponent Na alloying reactions with metals, and mirrors such reactions in Li cells. The carbon assists in the electrode electronic conductivity and mechanical stability while the Sn and Sb form a single SnSb phase that provides the very high capacities associated with alloying reactions. Typical volume changes of *ca*. 400% occur for the individual metals, but the nanocomposite SnSb/C can negotiate the volume change. In the proposed mechanism, the reaction of Na with the SnSb single phase occurs first making Na_3Sb and Sn (0.45 V discharge feature) followed by alloying of the Sn with Na at lower voltage (~0.2 V) to form $Na_{3.75}Sn$ in the nanocomposite. Reversible capacities of 544 mAh g^{-1} and Coulombic efficiencies above 98% were observed during cycling. The experimental capacity matches the theoretical value expected for a 1:1 molar Sn:Sb ratio, indicating that both metals are participating equally in the Na alloying reaction.

4. Electrolytes for Na-ion Batteries

Discovery of appropriate liquid electrolytes in conjunction with anode advances will also be necessary, and is a great opportunity for research. The most common electrolyte formulations for sodium batteries use either $NaPF_6$ or $NaClO_4$ as salts in carbonate ester solvents, particularly propylene carbonate (PC). Unfortunately, as mentioned previously, metallic sodium anodes corrode continuously in the presence of most commonly used organic electrolytes, rather than forming a stable solid electrolyte interphase (SEI). Highly reducing sodiated intercalation compounds intended for use as anodes may also require tailored SEIs to enable stable cycling in cells, similar to those that form on lithiated graphite electrodes in Li ion systems. Typical reduction products as impurities such as sodium propyl carbonate are generated at Na anode surfaces in reaction with PC, the most common solvent used in Na batteries. This species, can, in turn be oxidized at the opposite cathode at top-of-charge thereby limiting capacity utilization and causing Coulombic inefficiency. Formulations and conditions needed for proper SEI formation will need to be co-developed with anode materials to ensure success in the field. For example, recently, fluoroethylene carbonate (FEC) has been observed to form a passivating film (0.7 V reduction) on both carbon and native metallic sodium anodes thereby stabilizing the electrodes to further side reactions with solvents. Other additives, for instance, those used in Li-ion batteries such as vinylidene carbonate (VC), ethylene sulfite (ES), and *trans*-difluoroethylene carbonate (DFEC) were not effective, but improved cycling was seen for FEC at 10 vol.% for the carbon anode.[33] Another paper by Komaba *et al*. concludes, based on XPS and TOF-SIMS data, that the SEI film on hard carbon is largely inorganic salt based and contains precipitated species such as NaF on the surface (when $NaPF_6$ is used as electrolyte salt).[34] Earlier work by Thomas *et al*. using $NaClO_4$ in EC had shown that the SEI formed on carbon consists of Na_2CO_3 and sodium alkyl carbonates.[18] There is much research to be done on solvents, Na supporting electrolyte salts, and additives to understand the reaction mechanisms and enable stable cycling properties.

5. Na Battery Cathode Materials

For Na batteries, the cathode consists of a material that can accommodate Na cations reversibly at a voltage considered reasonably greater than 2 V positive to that of Na metal. Materials with lower voltages (< 2 V vs. Na) are best defined as anodes. The energy density of the Na battery can be maximized by increasing the working cathode voltage or decreasing the anode working potential, increasing specific electrode capacities and, in practice, producing materials with densely packed particles (high tap density). The use of Na metal as the counter electrode to screen conventionally loaded (active material 5–11 mg/cm^2) cathodes for more than *ca*. 50 cycles is difficult since Na metal plates unevenly and dendritically (even more so than Li) in organic electrolytes, thereby eliminating it as a viable long-term reversible counter electrode.

Cathodes for Na batteries work best if they function as a host material for Na; the volume change should be as negligible as possible for the material as it cycles Na in and out, and this capability is critical for long-term battery cycling performance. Not unexpectedly, materials with low volume change as a function of Na content tend to mimic structures common to those of Li-ion battery cathodes. Sodium prefers 6-coordination, either in an octahedral or prismatic arrangement, whereas Na tetrahedral coordination does not occur or is quite limited in

inorganic materials; this property inherently poses a limitation to the types of structures available for cathode materials. Poly-anionic networks that have available octahedral interstitials in their structures and layered oxide materials that have 2-D galleries present for holding Na cations in 6-coordinate geometry are the two major classes of cathode materials.

In contrast to anodes and electrolytes, cathode research in Na battery systems has already proven somewhat fruitful, with a number of transition metal oxide and poly-anionic compounds identified which look promising. Recent thermodynamic ab initio calculations for various cathode material structure types have been reported;[9] the energy difference between Li vs. Na was found to reduce the insertion potential for Na by 0.18 – 0.57 V compared to inserting Li in the same structure. The increased size and mass of the Na^+ ion compared to the Li^+ ion suggest that diffusion in similarly structured host materials will be slower for the former than for the latter, implying power restrictions in devices. Conversely, the same reference suggests that this may not be the case for layered sodium transition metal oxides compared to their Li counterparts: for alkali cobalt oxides the diffusion barrier for Na^+ system is lower than for Li^+. More work is needed to understand this phenomenon, but nevertheless, these calculations shows enticing promise for such materials and the power that can be delivered. In addition, we must not discount nanostructuring approaches for Na-ion electrodes, along the lines of those recently developed for olivine electrodes in lithium ion batteries, which should alleviate diffusion and electronic conductivity limitations. This is an example of how technology developed initially for lithium ion batteries can be leveraged to ensure rapid deployment of the sodium ion analogs.

5.1. Sulfides

Layered sulfides possess large galleries for intercalation of Na cations. Early work was directed primarily to binary metal sulfides, most famously, the canonical intercalation electrode, TiS_2.[35,36] The Ti(IV)/(III) redox couple is about 1.8–2.0 V vs. Na, and is about 0.3 V lower that the corresponding $LiTiS_2$ system. The advent of new layered oxides and recently reported framework poly-anionic cathodes provides much larger working voltages (>2.0 V) for Na cells compared to Na_xTiS_2. Other sulfides for ambient temperature non-aqueous Na batteries typically possess lower voltage, and are considered best as anodes; some examples include Ni_3S_2 (0.8 V vs. Na),[37] and Cu_2S (~1.0 V vs. Na).[38]

5.2. Fluorides

Perovskite transition metal fluorides (typically FeF_3) have been evaluated for their performance in Na batteries. When the Na reacts electrochemically with the material it fills the A site in the ABO_3 perovskite structure, and the Fe is reduced to Fe(II). The voltage at which this process occurs is approximately 2 V vs. Na.[39] There is a large hysteresis in the voltage curve, but the capacity can reach 240 $mAhg^{-1}$ at a low current rate of 0.2 mA cm^{-2}. It is also critical to ball mill the FeF_3 to small particle sizes to promote electrochemical reactivity. This material as prepared is in the charged state, so subsequent work focused on $NaFeF_3$ that is chemically synthesized in the discharged state using a solution phase nanomaterial synthesis.[40] $NaFeF_3$ as a discharge material in a Na cell indeed can be charged first to 4.5 V, then cycled reasonably between 1.5 and 4.5 V.

5.3. Phosphates and Sulfates

As documented in the literature for Li-ion batteries, Li transition metal phosphates with the olivine structure ($LiFePO_4$) have been widely reported and subsequently used throughout the battery industry following the critical discovery that these materials are electroactive by Padhi et al.[41] The lack of studies on the sodium-ion electrochemistry of sodium transition-metal phosphates for Na batteries is disappointing despite a large number of these phases having been synthesized. Many of these studies, instead, only considered electrochemical ion-exchange of the Na with Li inside Li-ion cells, and subsequent testing in Li batteries. However, electrochemical characterization of $NaFePO_4$ with the metastable olivine structure in Na cells has been recently reported.[42] Nearly all of the Na can be reversibly cycled from this structure and a practical capacity of 140 mAh g^{-1} was demonstrated. There are virtually no studies of phosphates in truly non-aqueous liquid *Na-ion* cells (*sans* metallic Na), apart from the pioneering work by Barker et al. on $NaVPO_4F$ coupled with a hard carbon anode.[43]

Nazar et al. have also examined cathodes in this class, synthesized using an interesting topochemical reaction from the ammonium cation precursor $NH_4MPO_4 \cdot H_2O$ (M = Fe, Ca, Mg).[44] Unfortunately, substitution of iron in this structure results in reduced electrochemical performance and only 0.6 Na could be cycled in $NaMn_{1/2}Fe_{1/2}PO_4$, corresponding to a specific capacity of 93 mAh g^{-1}. Recham et al. also noticed deleterious effects from substituting manganese for iron in Na_2FePO_4F; in this study, the poor conductivity of the oxyanion cathode materials was addressed using an ionothermal synthesis to make nanosized particles with better performance in Na cells than micron sized particles. These materials showed capacities of 110 mAh g^{-1}.[45]

While the class of NASICONS ($A_nM_2(XO_4)_3$); X = Si^{4+}, P^{5+}, S^{6+}, Mo^{6+}, As^{5+}, and so on), and their structures are well known for being used as Na ion conductors, their use as cathodes in Na cells is scarce. There is a single report from Plashnitsa et al. describing the use of $Na_3V_2(PO_4)_3$ using $NaClO_4$ in PC or an ionic liquid electrolyte ($NaBF_4$ in 1-ethyl-3-methyl imidazolium BF_4); both the V(III/IV) process at 3.4 V and V(II/III) at 1.2 V were observed although reversibility was poor, especially for the lower potential reaction.[46] Sodium transition metal sulfate fluorides, $NaMSO_4F$, which also exhibit high Na^+ ionic conductivity, have been tested for their electrochemical activity in Na cells. The parent iron compound (M = Fe) shows some redox activity at 3.6 V, but less than 0.1 Na could be reversibly inserted after charging to 4.2 V; other members of the series M = Mn, Co, Ni showed no evidence of sodium extraction.[47] However, Nazar *et al.* reported that after more vigorous charging conditions (extended potentiostatic charging at 4.5 V) approximately 0.6 Na could be reinserted in $NaFeSO_4F$, albeit with quite large

irreversible capacity.[48] A recent report also found no Na intercalation chemistry in these structures for M = Mg, Co, Ni, Cu, Zn.[49] Although these materials possess high Na^+ conductivity, Na removal from their structures appears to be energetically unfavorable.

A number of the more cyclable versions in Na cells contain V; $NaVPO_4F$ (80 mAh g^{-1}),[43] $Na_{1.5}VOPO_4F_{0.5}/C$ (composite) (87 mAh g^{-1}),[50] and the NASICON $Na_3V_2(PO_4)_3$ (120 mAh g^{-1}).[46] However, since vanadium is considered a toxic element, it may likely not find any use in practical applications. Therefore polyanion systems that focus on Mn, Fe, or mixed versions are the most desirable from an environmental and raw material cost perspective. Their use in Na cells and the possibility to tune the redox voltage based on the inductive effect of the metals involved is a good approach to improved materials. However, one must develop simple synthesis routes, and likely will need to use nanosizing and carbon coating processes (analogous to olivine $LiFePO_4$ in Li cells) in order to make these materials commercially viable. A recent review discussed phosphate materials in sodium-ion batteries and we direct the reader there for a more detailed discussion of these structures.[51]

5.4. Oxides

5.4.1. $Na_{0.44}MnO_2$ Tunnel Structure Oxides

Orthorhombic $Na_{0.44}MnO_2$ (*i.e.* $Na_4Mn_9O_{18}$) has large S-shaped tunnel structures and is electrochemically active to reversible Na electrochemical reaction as shown by Sauvage, et al.[52] and the earlier work of Doeff in Na-metal polymer cells.[53] The open framework allows Na^+ to cycle into and out of available octahedral sites with relative ease. Although this compound can provide relatively high capacity due to cycling *ca.* 0.6 Na (160 mAh g^{-1}), this full capacity is only accessible in half-cells where the extra Na not present in the starting material is provided by the anode. A revisit of $Na_{0.44}MO_2$ oxides in the form of nanowires was recently reported for Na batteries.[54] Although the specific capacity of 128 mAh g^{-1} was lower than previous reports for this material, the combination of the high-aspect ratio active nanomaterial with low electrode loading (~2 mg cm^{-2}) improved rates and provided remarkable capacity retention (77% after 1000 cycles at 0.5 C), thus demonstrating the effectiveness of nanosizing for Na electrochemical systems.

Some early work on the sodium insertion into the spinel λ-MnO_2 showed that the material converts to other MnO_2 structures, including $Na_{0.44}MnO_2$ and the layered $Na_{0.7}MnO_2$, during cycling.[55] A total rearrangement of the oxide lattice framework has to take place in order to accommodate Na in these structures since Na will not fit into the spinel tetrahedral sites.

5.4.2. Vanadium Oxides And Iron Oxides

Vanadium oxides with layered (α-V_2O_5 and $Na_{1+x}V_3O_8$) or tunnel (β-$Na_xV_2O_5$) structures have been demonstrated to reversibly cycle up to 1.6 Na (225 mAh g^{-1}), although the average cell potential is low and capacity retention is poor.[56,57] In contrast, Tepavcevic et al. reported that electrodeposited V_2O_5 achieved very high capacity (250 mAh g^{-1}) in Na cells for more than 300 cycles.[58] This nanostructured material reversibly converts between a disordered, cantilevered form in the deintercalated state to a bilayered structure when Na is inserted. $Na_{0.33}V_2O_5$ nanorods have also been tested as cathodes in Na cells, providing 142 mAh g^{-1}.[59] However, the complication associated with these vanadium oxides is that they are intrinsically synthesized in the charged state. Therefore, a source of sodium in the cell is necessary for these cathodes to operate effectively in a Na-ion format. Sodium vanadium oxides prepared in the discharged state, such as the layered oxides Na_xVO_2 (x = 0.7, 1) are also reported to cycle *ca.* 0.5 Na reversibly (130 mAh g^{-1}).[60,61] Voltage profiles indicate that sodium vacancy ordering occurs in the layer as a function of Na content, and this phenomena creates two-phase and solid-solution regions indicative in the voltage profiles.

Iron oxides that are synthesized in a nanoscale form show electrochemical reactivity at lower voltages when paired with Na metal as the counter electrode. For example, nanocrystalline (10 nm) Fe_3O_4 inverse spinel demonstrated between 110 and 160 mAh g^{-1} at about an average voltage of 1.8 V vs. Na.[62] The low voltage reactions are ascribed to the redox couple of Fe(III)/(II) in these oxides. A follow-on study of nanocrystallized Fe_3O_4 as well as α-Fe_2O_3 reported rechargeable capacities of 160 or 170 mAh g^{-1}, respectively, in the large voltage window of 1 to 4 V.[63]

5.4.3. Layered Sodium Transition-Metal Oxides

Two-dimensional lamellar oxides are the most important class of cathode materials as evidenced by their dominance in commercial high energy density Li-ion cells. Sodium analogues exist for virtually all of the layered lithium transition metal oxides. Layered AMO_2 (A = alkali, M = transition metal) compounds frequently exhibit differing electrochemical behavior in Na-ion vs. Li-ion systems. Although similar, there are subtle structural differences, owing to the larger size of Na, which limits cation disorder and prevents Na from occupying tetrahedral sites. The intercalation chemistry of Na^+ in these compounds has been studied more extensively than any other cathode class.

The structures of the layered ternary sodium transition-metal oxides were fully elaborated in the 1970's. The intercalation chemistry of these structures containing first-row late transition metals was originally studied in the context of the effects of Na removal on structure; typically they only examined potential windows in which Na cycling in the structure is highly reversible and thus the reported capacities are significantly lower than more recent re-examinations of such compounds. Much of the pioneering work came from research by Hagenmuller et al. and specialized nomenclature to describe the stacking arrangements of layered transition metal oxides was introduced by Delmas and Hagenmuller.[64] The coordination environment of the alkali metal is indicated by either P for prismatic coordination or O for octahedral, followed by a number describing the number of transition metal layers in the stacking repeat unit. It is common for monoclinic distortions of these structures to occur, in which case the letter describing the coordination of the alkali is appended with an apostrophe to denote the structural modification. Note that there are two independent sites for Na

in stacked prismatic coordination: one is shared between equal faces above and below the layer, while the second one is shifted by one octahedral group face directly next to the first.

P2 structures generally form at synthesis temperatures above 700 °C, while P3 forms dominate below 700 °C; the product structure also depends on the composition and the method of synthesis. Complicated P2/P3 intergrowths have resulted from slow cooling conditions, while P2 (or very close to P2) seems to prefer to form regardless of the composition and/or substitutions (i.e. Ni, Co, Al, etc.) when such materials are quenched from high temperature (above 800 °C). Note that the formation of oxygen vacancies is a frequent complication in the synthesis of some of these layered oxides (e.g., for Co and Mn). The non-stoichiometry of oxygen is difficult to determine directly and has a significant influence on electrochemical properties.[65,66] The structure is also affected by the interplay of charge ordering in the transition metal plane and Na vacancy ordering in the alkali layer. The greater the content of Na in the layer, the more preference there is for Na octahedral coordination, while the lower Na compositions systems tend towards Na prismatic coordination.[67]

The sodium cobaltate $NaCoO_2$ was the first to be examined for electrochemical sodium intercalation chemistry[68] and this compound has received a great deal of attention in other areas of research due to its interesting superconducting, thermoelectric, and magnetic properties.[69–71] The initial studies demonstrated that the various Na_xCoO_2 polymorphs could reversibly intercalate Na^+ over a limited range, with the P2 structure giving the highest capacity of 95 mAh g^{-1}.[72] The O3, O'3, and P'3 structures were shown to reversibly interconvert when Na^+ is electrochemically or chemically de-intercalated from $NaCoO_2$. Numerous two-phase regions were noted in the potential curve due to ordering in the Na plane and changes in coordination geometry there (O ↔ P transitions).[73] The transition from the other structures to P2 is difficult for layered oxides and would involve a rotation of the CoO_6 octahedra and Co-O bond-breaking, whereas transitions between P'3, O2, and O'3 only involve low-energy gliding of the transition metal slabs relative to one another. Shacklette also examined the series of Na_xCoO_2 compounds and found that the P2 polymorph has the best capacity retention, probably due to the lack of gross structural changes during cycling.[74] In the early 1990's Ma *et al.* built what were probably the first Na-ion secondary cells (*i.e.* not using Na metal) with $Na_{0.7}CoO_2$ against $Na_{15}Pb_4$ alloy anodes using a polymer electrolyte.[75]

Layered sodium iron oxides ($NaFeO_2$) and sodium manganese oxides ($NaMnO_2$) are attractive since they consist of elements that are inexpensive and relatively non-toxic. Implementation of $NaFeO_2$ in Na batteries has been limited, due to poor electrochemical properties. While α-$NaFeO_2$ is the structural prototype for layered materials in the *R-3m* space group, its performance in a Na cell is hindered by the unstable Fe(IV) oxidation state. Only the removal of Na has been shown to be possible, Na reinsertion has not been demonstrated; studies that used chemical deintercalation found that removal of even small amounts of sodium ($\Delta Na < 0.1$) from this compound leads to structural deterioration.[76,77] Electrochemical deintercalation was also used; in this case removal of more than 0.5 Na led to deleterious structural changes.[78]

The sodium manganese bronzes were studied very early on for their Na hosting abilities. As with the analogous Co structures, the P2-$Na_{0.7}MnO_{2.25}$ exhibited the highest reversible sodium activity of 96 mAh g^{-1} after charging to 3.5 V.[79] Later studies demonstrated that charging to higher potential (3.8 V) allowed higher reversible capacities at the expense of cycle life. Essentially complete cycling of the sodium in $Na_{0.6}MnO_2$, corresponding to 140 mAh g^{-1}, was reported by Caballero *et al.*[80] A more recent report from the Ceder group showed that using an analogue with higher initial sodium content (α-$NaMnO_2$), it is possible to cycle 0.75 Na in the structure (185 mAh g^{-1}) albeit with rapid capacity fade.[81]

Sodium chromium oxides ($NaCrO_2$), originally evaluated in a Na cell by Hagenmuller, suffered electrochemical instability due to Cr(IV) upon charge.[82] Komaba *et al.* later showed that $NaCrO_2$ can cycle 0.4 Na reversibly which is consistent with a capacity of 100 mAh g^{-1}.[83] Additionally they highlight a significant difference in Na vs. Li ion intercalation in this system. Compared to $LiCrO_2$, which does not reinsert Li after oxidation due to the movement of Cr(VI) to a vacant T_d site, as Na is removed from this structure, the Cr stays locked in place in the transition metal layer. Based on magnetism measurements, the authors surmised that only Cr(IV) is formed in the sodium system and thus the reversibility of the cell is good. This Na_xCrO_2 system was also recently studied by Xia and Dahn for evaluation of its thermal stability in the charged state ($x = 0.5$) using accelerating rate calorimetry (ARC).[84] These tests determined that $Na_{0.5}CrO_2$ is more stable than both delithiated $Li_{0.5}CoO_2$, and Li_0FePO_4 in the 1 M $NaPF_6$ in ethylene carbonate: diethyl carbonate (1:2) electrolyte. The stability is attributed to a lack of oxygen release from $Na_{0.5}CrO_2$; instead, disproportionation occurs to stoichiometric $NaCrO_2$ and a very slightly oxygen deficient $CrO_{2-\delta}$ phase. The virtual lack of thermal decomposition and heat generation as demonstrated by the ARC test to 350 °C may serve well the safety of Na batteries. More tests on other non-Cr layered oxides are needed to further examine this possibility.

Non-first row transition metal oxides of sodium also form layered structures and there is at least one example of reversible sodium intercalation. Electrochemical cycling of a material, $Na_xMo_2O_4$, indicated that the sodium intercalation process in $Na_xMo_2O_4$ is reversible within the range of composition $0.55 < x < 1.9$ with five single phase domains (evidenced by voltage plateaus) during desodiation.[85] This corresponds to a specific capacity of *ca.* 130 mAh g^{-1} but with an average cell potential of 1.8 V, too low for practical operation as a cathode for Na batteries.

The number of known Na-containing layered oxide materials expanded rapidly as the Li-ion battery field quickly developed in the 1990s. This interest was mainly driven by the use of the Na compounds as precursors to metastable Li polymorphs that could not be synthesized by direct solid state chemistry. Bruce[86] and Delmas[87] took the corresponding Na precursors $NaMnO_2$ and converted them to the layered Li analogs $LiMnO_2$ through low-temperature ion-exchange reactions thus producing new Li battery cathodes. A wide variety of substituted compounds were synthesized in this way for the express purpose of ion-exchanging the Na for Li and in most cases, the Na electrochemistry was not examined.[88,89] As with layered lithium cathode

materials, the occupants of the transition metal plane can be varied to tune properties and the most useful materials result from combinations of different transition metals. The first example in this vein came from Saadoune *et al*. who examined electrochemical sodium insertion of $Na_{0.58}Ni_{0.6}Co_{0.4}O_2$, but only demonstrated the reinsertion of 0.4 Na into the structure.[90] The $Na_{2/3}Mn_{2/3}Ni_{1/3}O_2$ system examined by Dahn's group was shown to be capable of cycling almost all of the sodium in the structure, providing capacities of 150-160 mAh g^{-1}, but only two cycles were demonstrated, so the long term cyclability of this compound is not known. A $Na_{2/3}Mn_{1/3}Co_{2/3}O_2$ phase has also been reported by Carlier *et al*. as being capable of cycling 0.45 Na giving a capacity of 115 mAh g^{-1}, but again, only 2 cycles were shown.[91]

The $NaNi_{1/2}Mn_{1/2}O_2$ system reported by Komaba and co-workers is the most extensively studied layered sodium compound in terms of its capabilities as a cathode in sodium batteries. The material demonstrates decent reversibility in the potential range of 2 to 3.8 V, delivering *ca*. 120 mAh g^{-1} for at least 15 cycles; charging to 4.5 V subsequently allowed reinsertion of 0.77 Na (185 mAh g^{-1}), but with a large irreversible capacity.[83] Subsequently, they have extended the application of this material towards advanced sodium-ion systems. Full cell designs using hard carbon anodes and the performance enhancing effects of FEC as an electrolyte additive in this system have been demonstrated.[33,34]

Johnson's group has described a Li-containing P2 layered $Na_{1.0}Li_{0.2}Ni_{0.25}Mn_{0.75}O_y$ oxide composition prepared from a conventional solid state reaction at 850 °C.[92] Layered Na P2 structures result despite slow-cooling, along with small amounts of a layered Li phase. The high concentration of Li in the material was used in order to create a favorable Li-Mn electronic interaction and $LiMn_6$ structural motif similar to that found in Li-rich Li-Ni-Mn oxides. It appears that Li resides in multiple sites based on preliminary ^{6}Li MAS NMR studies. The electrochemical performance in Na-metal cells showed reversible capacities of 100 mAh g^{-1} with good rate capability, retaining 80% of this capacity at a 10 C rate. From *ex situ* XRD data, it appears that no gliding of transition metal slabs occurs and the material retains P2 throughout cycling. The electrochemical activity in the potential range of 2 – 4.2 V vs. Na/Na^+ only involves Ni(II/IV) redox, as indicated by in situ XANES analysis. The Mn redox state remains silent as 4+ and there is no distortion around the Mn metal center. Our group has also recently described the *R-3m* compound $Na(Mn_{1/3}Fe_{1/3}Ni_{1/3})O_2$ which can provide 120 mAh g^{-1} in half-cells in the potential range of 2–4 V;[12] the mechanism of charge compensation in this material has not yet been elucidated. Full cell designs with hard carbon anodes delivered good performance with over 150 cycles at 0.5 C.

For most of the layered compounds described above, only about 0.5 Na can be cycled in the structure, delivering capacities of *ca*. 120 mAh g^{-1} or less at average potentials of 3.5 V, indicating that there is significant room for improvement in the specific capacities of these materials; although over extraction of Na has been shown to cause structural degradation in some layered oxides, capacities must be improved if these materials are to find practical implementation. We have recently achieved high reversible capacity from $Na_{0.6}Li_{0.6}Ni_{0.25}Mn_{0.75}O_y$ in Na metal cells by charging to high potential, as shown in Figure 10, presumably removing a large portion of Li from the structure. That the materials exhibit stable high-capacity cycling after near-complete electrochemical oxidation hints at structural stabilization by residual Li and we are currently in the process of detailed structural characterization of this system.

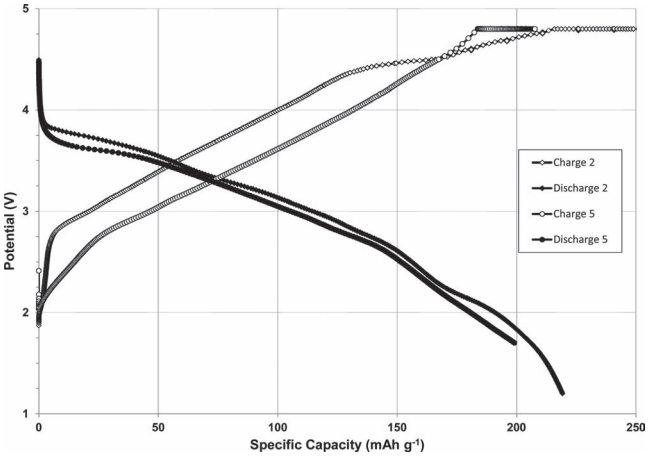

Figure 10. Na || $Na_{0.6}Li_{0.6}Ni_{0.25}Mn_{0.75}O_y$ with 1 M $NaPF_6$ in PC electrolyte provides 200 mAh g^{-1} after charging to 4.8 V.

6. Conclusions

Na-ion based electrochemical energy storage is a complementary alternative to Li-ion based systems. The main advantage that can be pressed with non-aqueous Na-ion chemistry is lower material cost than for Li based systems, although the practical utility of commercial Na-ion implementation will depend on the Li market. A renewal in interest for Na-ion systems has resulted in a number of new materials being reported recently and performance in some cases is similar to early Li-ion technology. With the improvements in cell-design and electrode engineering that have been made in the advancement of Li-ion batteries, it may be of interest to reinvestigate older Na electrode materials for their performance in Na cells.

7. Experimental Section

Synthesis of cathode active materials: Sodium-ion cathode materials used in this work were prepared as described previously.[92]

Preparation of laminate electrodes: Cathode laminates were prepared by blade casting of slurries of the active material (82%w/w), Super-P Li carbon black (Timcal) (8%w/w), and pVDF binder (Arkema) (8%w/w) in N-methyl pyrrolidinone onto Al-foil current collectors. Anode laminates were prepared in a similar manner using carbon active material (92%w/w) and pVDF (8%w/w) on Cu foil.

Preparation of tin electrodes: Tin was conformally plated onto a copper substrate using a commercial electroless plating bath (Caswell) with an immersion time of 1 min.

Electrochemical testing: All electrochemical testing was performed in 2032 coin cell hardware (Hohsen). 1 mol dm^{-3} $NaClO_4$ or $NaPF_6$ in PC electrolytes were used with Whatman GF/F glass fiber separators. Sodium metal foil anodes were prepared from sodium metal chunks by cutting away the oxidized surface and pressing to a thin foil by hand. All cells were assembled in an inert atmosphere glovebox (<1 ppm O_2).

Acknowledgements

Funding from the Department of Energy under Contract DE-AC02-06CH11357 is gratefully acknowledged. The authors would like to thank V.A. Maroni for Raman measurement of carbon. The use of Raman instrumentation at Argonne's Center for Nanoscale Materials was supported by the US DOE, Office of Science, Office of Basic Energy Sciences. In addition we would like to thank Marca Doeff, Kevin Gallagher, Jack Vaughey, Shawn Rood, Lynn Trahey, and Haiming Wen for helpful discussions.

Received: March 13, 2012
Published online: May 21, 2012

[1] J. Akridge, R. Brodd, Pacific Power Symposium, Waikoloa, Hawaii **2010**.
[2] "Lithium" in *Mineral Commodity Summaries 2012*, U.S. Geological Survey, Reston, VA, **2012**, p. 94.
[3] "Market," *The Lithium Site*, 2012, http://www.lithiumsite.com/market.html. (Accessed February 2012).
[4] Research Center for Energy Economics: http://www.ffe.de/en (Accessed February 2012).
[5] "Soda Ash" in *Mineral Commodity Summaries 2012*, U.S. Geological Survey, Reston, VA, 2012, p. 148.
[6] Z. Yang, J. Zhang, M. C. W. Kintner-Meyer, X. Lu, D. Choi, J. P. Lemmon, J. Liu, *Chem. Rev.* **2011**, *111*, 3577.
[7] C. Wadia, P. Albertus, V. Srinivasan, *J. Power Sources* **2011**, *196*, 1593.
[8] T. B. Reddy, D. Linden, *Linden's Handbook of Batteries*, McGraw-Hill, **2010**.
[9] S. P. Ong, V. L. Chevrier, G. Hautier, A. Jain, C. Moore, S. Kim, X. Ma, G. Ceder, *Energy Environ. Sci.* **2011**, *4*, 3680.
[10] P. A. Nelson, K. G. Gallagher, I. Bloom, D. W. Dees, *"Modeling the Performance and Cost of Lithium-Ion Batteries for Electric Vehicles"* Chemical Sciences and Engineering Division, Argonne National Laboratory, ANL-11/32, Argonne, IL USA **2011**.
[11] V. L. Chevrier, G. Ceder, *J. Electrochem. Soc.* **2011**, *158*, A1011.
[12] D. Kim, E. Lee, M. Slater, W. Lu, S. Rood, C. S. Johnson, *Electrochem. Commun.* **2012**.
[13] P. Ge, M. Fouletier, *Solid State Ionics* **1988**, *28–30*, 1172.
[14] M. M. Doeff, Y. Ma, S. J. Visco, L. C. De Jonghe, *J. Electrochem. Soc.* **1993**, *140*, L169.
[15] R. Alcantara, J. M. J. Mateos, J. L. Tirado, *J. Electrochem. Soc.* **2002**, *149*, A201.
[16] E. Zhecheva, R. Stoyanova, J. M. Jiménez-Mateos, R. Alcántara, P. Lavela, J. L. Tirado, *Carbon* **2002**, *40*, 2301.
[17] R. Alcántara, J. M. Jiménez-Mateos, P. Lavela, J. L. Tirado, *Electrochem. Commun.* **2001**, *3*, 639.
[18] P. Thomas, J. Ghanbaja, D. Billaud, *Electrochim. Acta* **1999**, *45*, 423.
[19] M. Dubois, D. Billaud, *Electrochim. Acta* **2002**, *47*, 4459.
[20] M. Dubois, A. Naji, D. Billaud, *Electrochim. Acta* **2001**, *46*, 4301.
[21] D. A. Stevens, J. R. Dahn, *J. Electrochem. Soc.* **2001**, *148*, A803.
[22] D. A. Stevens, J. R. Dahn, *J. Electrochem. Soc.* **2000**, *147*, 4428.
[23] L. Joncourt, M. Mermoux, P. H. Touzain, L. Bonnetain, D. Dumas, B. Allard, *J. Phys. Chem. Solids* **1996**, *57*, 877.
[24] X. Xia, J. R. Dahn, *J. Electrochem. Soc.* **2012**, *159*, A515.
[25] R. Alcantara, P. Lavela, G. F. Ortiz, J. L. Tirado, *Electrochem. Solid-State Lett.* **2005**, *8*, A222.
[26] D. A. Stevens, J. R. Dahn, *J. Electrochem. Soc.* **2000**, *147*, 1271.
[27] S. Wenzel, T. Hara, J. Janek, P. Adelhelm, *Energy & Environ. Sci.* **2011**.
[28] P. Senguttuvan, G. l. Rousse, V. Seznec, J.-M. Tarascon, M. R. Palacín, *Chem. Mater.* **2011**, *23*, 4109.
[29] H. Xiong, M. D. Slater, M. Balasubramanian, C. S. Johnson, T. Rajh, *J. Phys. Chem. Lett.* **2011**, *2*, 2560.
[30] R. Alcántara, M. Jaraba, P. Lavela, J. L. Tirado, *Chem. Mater.* **2002**, *14*, 2847.
[31] Q. Sun, Q.-Q. Ren, H. Li, Z.-W. Fu, *Electrochem. Commun.* **2011**, *13*, 1462.
[32] L. Xiao, Y. Cao, J. Xiao, W. Wang, L. Kovarik, Z. Nie, J. Liu, *Chem. Commun.* **2012**.
[33] S. Komaba, T. Ishikawa, N. Yabuuchi, W. Murata, A. Ito, Y. Ohsawa, *ACS Appl. Mater. Interfaces* **2011**, *3*, 4165.
[34] S. Komaba, W. Murata, T. Ishikawa, N. Yabuuchi, T. Ozeki, T. Nakayama, A. Ogata, K. Gotoh, K. Fujiwara, *Adv. Funct. Mater.* **2011**, *21*, 3859.
[35] M. S. Whittingham, *Prog. Solid State Chem.* **1978**, *12*, 41.
[36] K. M. Abraham, *Solid State Ionics* **1982**, *7*, 199.
[37] J.-S. Kim, H.-J. Ahn, H.-S. Ryu, D.-J. Kim, G.-B. Cho, K.-W. Kim, T.-H. Nam, J. H. Ahn, *J. Power Sources* **2008**, *178*, 852.
[38] J.-S. Kim, D.-Y. Kim, G.-B. Cho, T.-H. Nam, K.-W. Kim, H.-S. Ryu, J.-H. Ahn, H.-J. Ahn, *J. Power Sources* **2009**, *189*, 864.
[39] M. Nishijima, I. D. Gocheva, S. Okada, T. Doi, J.-i. Yamaki, T. Nishida, *J. Power Sources* **2009**, *190*, 558.
[40] Y. Yamada, T. Doi, I. Tanaka, S. Okada, J.-i. Yamaki, *J. Power Sources* **2011**, *196*, 4837.
[41] A. K. Padhi, K. S. Nanjundaswamy, J. B. Goodenough, *J. Electrochem. Soc.* **1997**, *144*, 1188.
[42] P. Moreau, D. Guyomard, J. Gaubicher, F. Boucher, *Chem. Mater.* **2010**, *22*, 4126.
[43] J. Barker, M. Y. Saidi, J. L. Swoyer, *Electrochem. Solid-State Lett.* **2003**, *6*, A1.
[44] K. T. Lee, T. N. Ramesh, F. Nan, G. Botton, L. F. Nazar, *Chem. Mater.* **2011**, *23*, 3593.
[45] N. Recham, J. N. Chotard, L. Dupont, K. Djellab, M. Armand, J. M. Tarascon, *J. Electrochem. Soc.* **2009**, *156*, A993.
[46] L. S. Plashnitsa, E. Kobayashi, Y. Noguchi, S. Okada, J.-i. Yamaki, *J. Electrochem. Soc.* **2010**, *157*, A536.
[47] P. Barpanda, J.-N. Chotard, N. Recham, C. Delacourt, M. Ati, L. Dupont, M. Armand, J.-M. Tarascon, *Inorg. Chem.* **2010**, *49*, 7401.
[48] R. Tripathi, T. N. Ramesh, B. L. Ellis, L. F. Nazar, *Angew. Chem., Int. Ed.* **2010**, *49*, 8738.
[49] M. Reynaud, P. Barpanda, G. Rousse, J.-N. Chotard, B. C. Melot, N. Recham, J.-M. Tarascon, *Solid State Sciences* **2012**, *14*, 15.
[50] F. Sauvage, E. Quarez, J. M. Tarascon, E. Baudrin, *Solid State Sci.* **2006**, *8*, 1215.
[51] V. Palomares, P. Serras, I. Villaluenga, K. Hueso, J. Carretero-González, T. Rojo *Energy Environ. Sci.* **2012**, *5*, 5884.
[52] F. Sauvage, L. Laffont, J. M. Tarascon, E. Baudrin, *Inorg. Chem.* **2007**, *46*, 3289.
[53] M. M. Doeff, M. Y. Peng, Y. Ma, L. C. De Jonghe, *J. Electrochem. Soc.* **1994**, *141*, L145.
[54] Y. Cao, L. Xiao, W. Wang, D. Choi, Z. Nie, J. Yu, L. V. Saraf, Z. Yang, J. Liu, *Adv. Mater.* **2011**, *23*, 3155.
[55] J. M. Tarascon, D. G. Guyomard, B. Wilkens, W. R. Mc Kinnon, P. Barboux, *Solid State Ionics* **1992**, *57*, 113.
[56] K. West, B. Zachau-Christiansen, T. Jacobsen, S. Skaarup, *Solid State Ionics* **1988**, *28–30*, *Part 2*, 1128.

[57] K. West, B. Zachau-Christiansen, T. Jacobsen, S. Skaarup, *J. Power Sources* **1989**, *26*, 341.
[58] S. Tepavcevic, H. Xiong, V. R. Stamenkovic, X. Zuo, M. Balasubramanian, V. B. Prakapenka, C. S. Johnson, T. Rajh, *ACS Nano* **2011**, *6*, 530.
[59] H. Liu, H. Zhou, L. Chen, Z. Tang, W. Yang, *J. Power Sources* **2011**, *196*, 814.
[60] D. Hamani, M. Ati, J.-M. Tarascon, P. Rozier, *Electrochem. Commun.* **2011**, *13*, 938.
[61] C. Didier, M. Guignard, C. Denage, O. Szajwaj, S. Ito, I. Saadoune, J. Darriet, C. Delmas, *Electrochem. Solid-State Lett.* **2011**, *14*, A75.
[62] S. Komaba, T. Mikumo, A. Ogata, *Electrochem. Commun.* **2008**, *10*, 1276.
[63] S. Komaba, T. Mikumo, N. Yabuuchi, A. Ogata, H. Yoshida, Y. Yamada, *J. Electrochem. Soc.* **2010**, *157*, A60.
[64] C. Delmas, C. Fouassier, P. Hagenmuller, *Physica B+C* **1980**, *99*, 81.
[65] J. Molenda, A. Stokłosa, D. Than, *Solid State Ionics* **1987**, *24*, 33.
[66] F. C. Chou, E. T. Abel, J. H. Cho, Y. S. Lee, *J. Phys. Chem. Solids* **2005**, *66*, 155.
[67] C. Fouassier, G. Matejka, J.-M. Reau, P. Hagenmuller, *J. Solid State Chem.* **1973**, *6*, 532.
[68] J.-J. Braconnier, C. Delmas, C. Fouassier, P. Hagenmuller, *Mater. Res. Bull.* **1980**, *15*, 1797.
[69] R. E. Schaak, T. Klimczuk, M. L. Foo, R. J. Cava, *Nature* **2003**, *424*, 527.
[70] M. Roger, D. J. P. Morris, D. A. Tennant, M. J. Gutmann, J. P. Goff, J. U. Hoffmann, R. Feyerherm, E. Dudzik, D. Prabhakaran, A. T. Boothroyd, N. Shannon, B. Lake, P. P. Deen, *Nature* **2007**, *445*, 631.
[71] M. Pollet, M. Blangero, J.-P. Doumerc, R. Decourt, D. Carlier, C. Denage, C. Delmas, *Inorg. Chem.* **2009**, *48*, 9671.
[72] C. Delmas, J.-J. Braconnier, C. Fouassier, P. Hagenmuller, *Solid State Ionics* **1981**, *3–4*, 165.
[73] R. Berthelot, D. Carlier, C. Delmas, *Nat. Mater.* **2011**, *10*, 74.
[74] L. W. Shacklette, T. R. Jow, L. Townsend, *J. Electrochem. Soc.* **1988**, *135*, 2669.
[75] Y. Ma, M. M. Doeff, S. J. Visco, L. C. De Jonghe, *J. Electrochem. Soc.* **1993**, *140*, 2726.
[76] S. Kikkawa, S. Miyazaki, M. Koizumi, *Mat. Res. Bull.* **1985**, *20*, 373.
[77] M. C. Blesa, E. Moran, C. León, J. Santamaria, J. D. Tornero, N. Menéndez, *Solid State Ionics* **1999**, *126*, 81.
[78] Y. Takeda, K. Nakahara, M. Nishijima, N. Imanishi, O. Yamamoto, M. Takano, R. Kanno, *Mat. Res. Bull.* **1994**, *29*, 659.
[79] A. Mendiboure, C. Delmas, P. Hagenmuller, *J. Solid State Chem.* **1985**, *57*, 323.
[80] A. Caballero, L. Hernán, J. Morales, L. Sánchez, J. Santos Peña, M. A. G. Aranda, *J. Mater. Chem.* **2002**, *12*, 1142.
[81] X. Ma, H. Chen, G. Ceder, *J. Electrochem. Soc.* **2011**, *12*, A1307.
[82] J. J. Braconnier, C. Delmas, P. Hagenmuller, *Mat. Res. Bull.* **1982**, *17*, 993.
[83] S. Komaba, T. Nakayama, A. Ogata, T. Shimizu, C. Takei, S. Takada, A. Hokura, I. Nakai, *ECS Trans.* **2009**, *16*, 43.
[84] X. Xia, J. R. Dahn, *Electrochem. Solid-State Lett.* **2012**, *15*, A1.
[85] J. M. Tarascon, G. W. Hull, *Solid State Ionics* **1986**, *22*, 85.
[86] A. R. Armstrong, P. G. Bruce, *Nature* **1996**, *381*, 499.
[87] F. Capitaine, P. Gravereau, C. Delmas, *Solid State Ionics* **1996**, *89*, 197.
[88] J. M. Paulsen, R. A. Donaberger, J. R. Dahn, *Chem. Mater.* **2000**, *12*, 2257.
[89] J. M. Paulsen, J. R. Dahn, *Solid State Ionics* **1999**, *126*, 3.
[90] I. Saadoune, A. Maazaz, M. Ménétrier, C. Delmas, *J. Solid State Chem.* **1996**, *122*, 111.
[91] D. Carlier, J. H. Cheng, R. Berthelot, M. Guignard, M. Yoncheva, R. Stoyanova, B. J. Hwang, C. Delmas, *Dalton Trans.* **2011**, *40*.
[92] D. Kim, S.-H. Kang, M. Slater, S. Rood, J. T. Vaughey, N. Karan, M. Balasubramanian, C. S. Johnson, *Adv. Energy Mater.* **2011**, *1*, 333.